Control of Current Waveform for Pulsed MIG Welding of Aluminum Alloy Sheets

Min Xu and Jiaxiang Xue

Abstract In this chapter, a simplified model of pulsed MIG welding is established and simulated using MATLAB. In addition, the anti-interference of a current waveform is simulated using the adaptive neural network feedforward control. Depending on the "one droplet per pulse" relationship in pulse frequency modulation, faster adjustment of the arc length, compared with the adjustment of the constant current characteristic, is achieved by increasing or decreasing the base time of the average current.

Keywords Aluminum alloy · Power supply for pulsed MIG welding
Adaptive neural network · One droplet per pulse

1 Introduction

The base current is the primary factor for maintaining an arc in the welding process, especially in the control of the low energy input of thin aluminum alloy pulsed MIG welding. To obtain the ideal base current and time, PID control is employed to achieve a steady arc and to not burn through the aluminum alloy sheet [1–3]. The required base current of pulsed welding is the object of this PID control.

M. Xu · J. Xue (✉)
School of Mechanical and Automotive Engineering,
South China University of Technology, Guangzhou, China
e-mail: mejiaxue@scut.edu.cn

S. Chen et al. (eds.), *Transactions on Intelligent Welding Manufacturing*,
Transactions on Intelligent Welding Manufacturing,
https://doi.org/10.1007/978-981-10-7043-3_12

2 PID Modeling and Control Simulation

2.1 Principle of PID Control

In 1922, the use of proportional integral derivative (PID) control [1] in the position control system was proposed by Nicholas Minorsky. The system block diagram is shown in Fig. 1.

The incremental PID control algorithm satisfies the DSP programming requirements and causes less error due to misoperation [2]. Therefore, in this chapter, the control algorithm is adopted; the subroutine flow chart is shown in Fig. 2. The formula is developed according to the following recursive principle:

$$u(k-1) = k_p\left(\mathrm{error}(k-1) + T_I\sum_{j=0}^{k-1}\mathrm{error}(j) + T_D(\mathrm{error}(k-1) - \mathrm{error}(k-2))\right)$$

The incremental PID control algorithm is as follows:

$$\begin{aligned}\Delta u(k) &= u(k) - u(k-1)\\ \Delta u(k) &= k_p(\mathrm{error}(k) - \mathrm{error}(k-1)) + T_I\mathrm{error}(k)\\ &\quad + T_D(\mathrm{error}(k) - 2\mathrm{error}(k-1) + \mathrm{error}(k-2))\end{aligned}$$

Taking into account the limits on word length and the operating speed of the program, the PID control algorithm is combined with the integer operation, but the operation results in error due to a half adjustment. To reduce the rounding error, the method of reducing the value of the coefficient k is proposed. It is worth noting that due to the reluctance of the k value within a certain range in an actual process, appropriate compensation for the remainder of k is needed. The operation process is shown in Fig. 3.

2.2 PID Controller Parameters

To obtain the ideal control effect, the optimal values of k_p, T_I, and T_D in the PID controller algorithm are determined based on a simulation; the simulation waveform

Fig. 1 Schematic diagram of PID control system

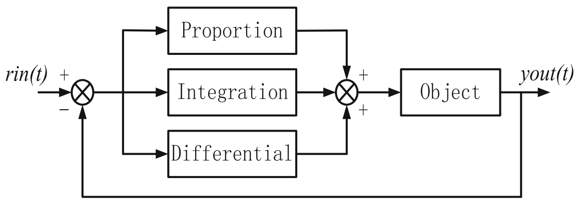

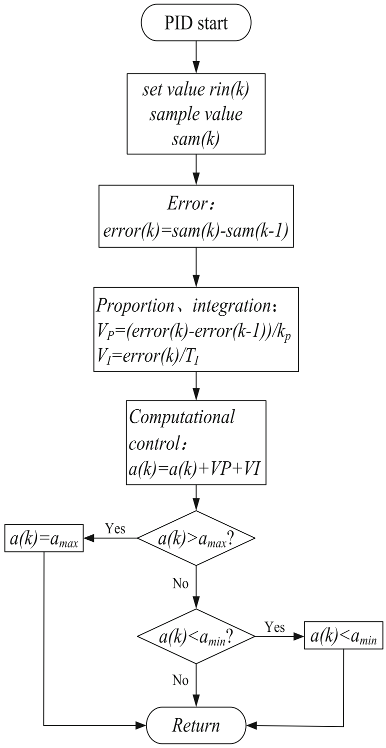

Fig. 2 Flow chart of PID control subroutine

of the pulse is shown in Fig. 4. The transfer function of the aluminum alloy pulsed MIG welding power supply is as follows [3]:

$$G(s) = \frac{1}{s^3 + 6s^2 + 5s}$$

While adjusting k_p, it is found, by comparing (a) and (b) in Fig. 5, that the smaller the value of k_p is, the less the number of shock waves is; hence, the best value of k_p to achieve the maximum output current is 2.2.

Mere adjustment of the k_p cannot lead to the desired outcome; therefore, the T_I value must be regulated after the k_p is determined. Figure 6 shows that the greater the value of T_I is, the smoother the waveform is and that the overshoot phenomenon eased significantly when k_p = 2.2, T_I = 3.

Finally, after the k_p and T_I values settle, the differential time T_D is employed to avoid the overshoot. Comparing the different results, T_D = 20 is determined to be the best T_D parameter, as shown in Fig. 7. To sum up, the best PID parameters suitable for this chapter are k_p = 2.2, T_I = 3, and T_D = 20.

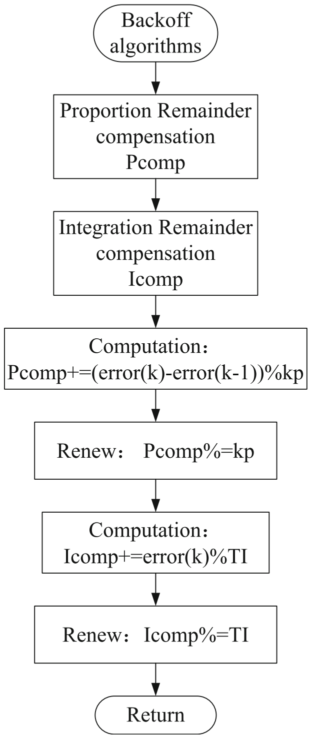

Fig. 3 Proportional and integral remainder error complement

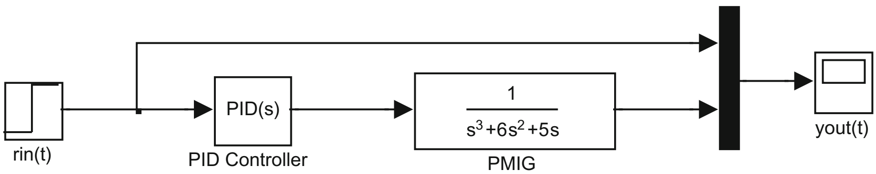

Fig. 4 PID controller parameter regulation simulation model

3 Anti-disturbance Control

The aluminum alloy pulsed MIG welding power supply is a piece of electrical equipment that combines strong and weak current; hence, there are multiple sources of interference, including the electromagnetic fields, the power grids, and the chip itself. The disturbance of the current signal, which is the foundation of the control, can be caused by the above sources of interference. Therefore, the suppression of interference signals is necessary in thin aluminum alloy pulsed MIG welding [4].

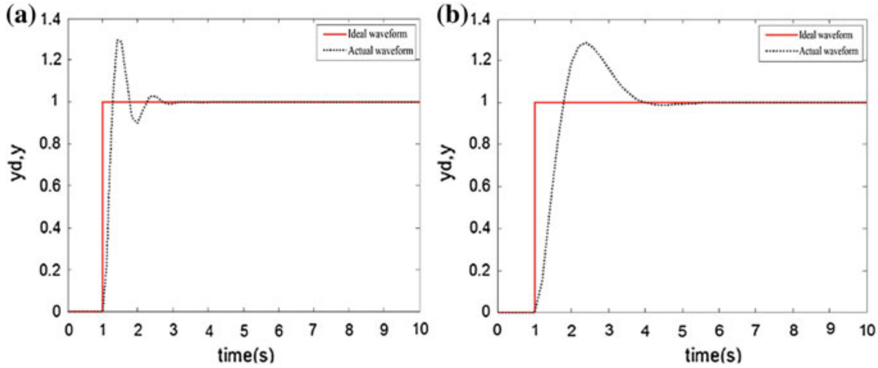

Fig. 5 k_p simulation diagram: **a** k_p = 10; **b** k_p = 3

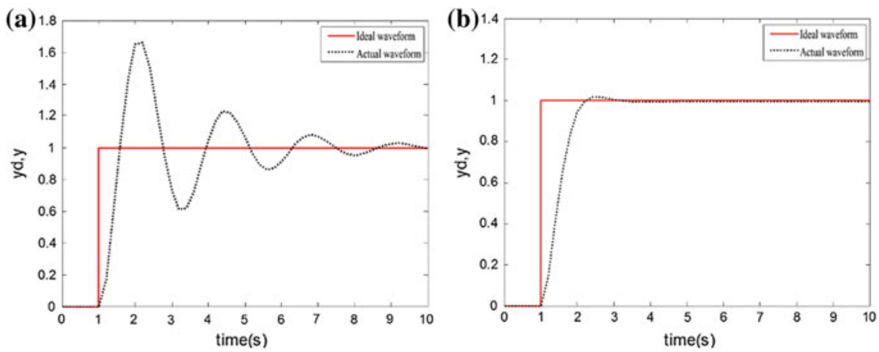

Fig. 6 T_{I} simulation diagram: **a** T_{I} = 10; **b** T_{I} = 4

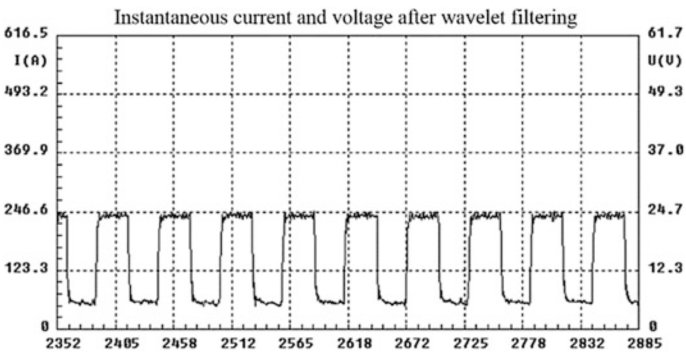

Fig. 7 Current output waveform corresponding to the best PID parameters

The traditional feedforward controller is based on the size and direction of the interference and is controlled by the interference so that the original object does not deviate [5].

According to Hecht Nielsen, the artificial neural network (ANN) is a large-scale nonlinear adaptive system composed of a number of processing units through a certain interconnection [6]. The artificial neural network can be used to address questions in cases with unknown background knowledge and inference rules because an ANN can offer distributed storage, parallel processing, self-learning, self-organizing, and adaptive nonlinear dynamic systems [7]. Therefore, in this chapter, the artificial neural network is used to replace the traditional feedforward compensator for feedforward control. The control structure model is shown in Fig. 8.

The pulsed MIG welding power supply of an alloy sheet [8] is equivalent to

$$M\dot{q} + F(q, \dot{q}) = u, \quad y = q + d$$

where M is the unknown system inertia, Q is the ideal output, that is, the external factors caused by the interference, D is the interference of the output of the system, u is the input of the system, and y is the output of the system.

The tracking error is expressed as $e_v = \dot{e} + \lambda_c e$ ($\lambda_c > 0$, a scalar), and the formulation can be expressed as:

$$\begin{aligned} M\dot{e}_v &= M\ddot{e} + M\lambda_c\dot{e} \\ &= F(q, \dot{q}) - u + M\ddot{q}_d + M\lambda_c\dot{e} - M\ddot{d} \end{aligned}$$

Hypothesis 1: Nominal control can guarantee the asymptotic convergence of the tracking error e_v, that is, the Lyapunov function

$$V_1(e_v) = \frac{1}{2}Me_v^2$$

Hypothesis 2: The optimal weight W_1 is specified on the compact set and is calculated by solving

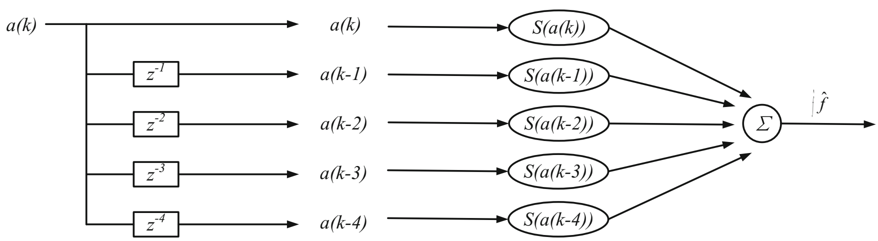

Fig. 8 Neural network compensation structure

$$M\dot{e}_v = F(q,\dot{q}) - u_{\text{nominal}} + \hat{w}^T\Phi(x) + M\ddot{q}_d + M\lambda_c\dot{e} - H(x) - \Delta\phi_1$$
$$= F(q,\dot{q}) - u_{\text{nominal}} + M\ddot{q}_d + M\lambda_c\dot{e} - \bar{w}^T\Phi(x) - \Delta\phi_1 - \Delta\phi_2$$

The weight estimation error is $\bar{w} = w - \hat{w}$. The corrected adaptive law [9–12], based on the parameter w, is as follows:

$$\dot{\hat{w}} = -\Gamma\Phi(x)e_v - \sigma\Gamma|e_v|\hat{w}$$

where $\Gamma > 0$ is the gain matrix; $\sigma > 0$ is a scalar parameter.

Theorem *Considering the control law, the parameter update method, and the tracking error, and taking the Lyapunov equation into account, the following calculation can be obtained:*

$$V = \frac{1}{2}Me_v^2 + \frac{1}{2}\bar{w}^T\Gamma^{-1}\bar{w}$$
$$|e| \le \frac{\varepsilon_1 + \varepsilon_2 + \frac{\sigma}{4}M^{*2}}{Q\lambda_c}$$

It can be seen that the system is stable.

4 Simulation Results and Analysis

The external disturbance transfer function is as follows:

$$D(s) = \frac{3.757\times10^{-6}s^3 + 0.3077s^2 + 1.381\times10^4 s + 8.374\times10^8}{s^3 + 1885s^2 + 1.777\times10^6 s + 8.374\times10^8}$$

The ideal waveform is selected as $q_d = 0$, $\dot{q}_d = 0$, $\ddot{q}_d = 0$. The external vibration $\omega = 0.2\sin500t$ is introduced at $t = 0$. The simulation uses the integral step $t_s = 1$, and its initial condition is that the nominal controller is PID controller 2. The structure of the controller is as follows:

$$u = u_{\text{nominal}} - w^{\mathrm{T}}\Phi(a(k), a(k-1), a(k-2), a(k-3), a(k-4))$$

Among them, $w = \begin{bmatrix} w_1 & w_2 & w_3 & w_4 & w_5 \end{bmatrix}^{\mathrm{T}}$, the basis function is $S(x) = 1.18/(1 + e - x)$, and the network basis function is

$$\Phi(a(k), a(k-1), a(k-2), a(k-3), a(k-4))$$
$$= [S(a(k), a(k-1), a(k-2), a(k-3), a(k-4))]^{\mathrm{T}}$$

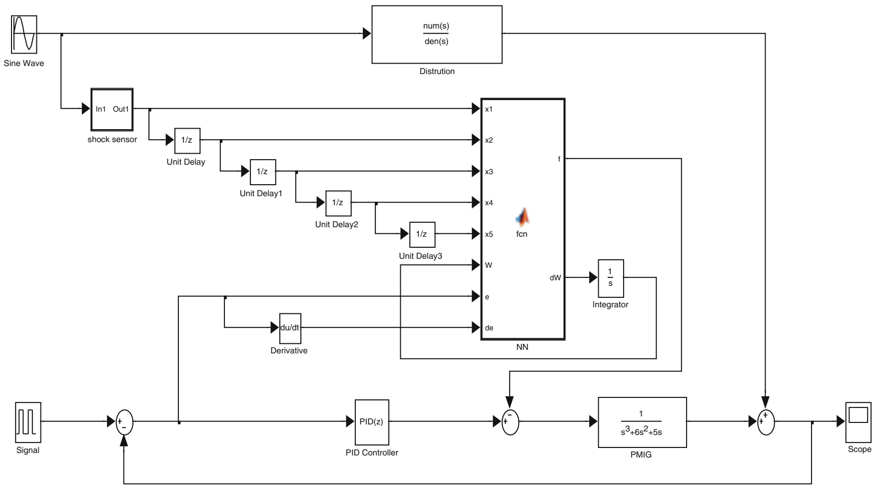

Fig. 9 Simulation of adaptive neural network feedforward control based on *e* correction

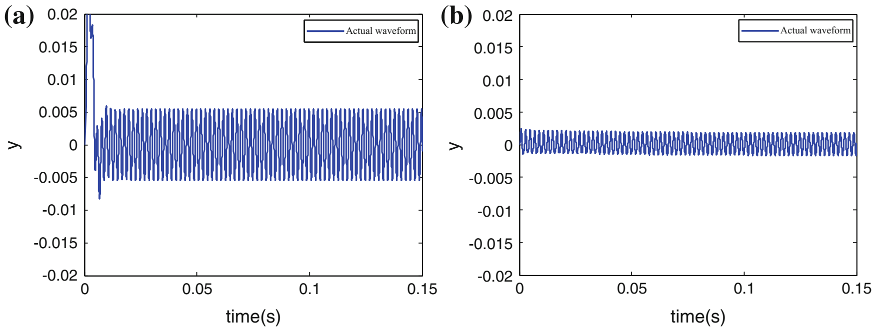

Fig. 10 Comparison of simulation waveforms: **a** Waveform with external disturbance. **b** Waveform diagram of adaptive neural network feedforward control based on *e* correction method

The tracking error expression $e_v = \dot{e} + \lambda_c e$, the feedforward input $f = w^{\mathrm{T}}\Phi(x)$ and the modified adaptive law are all included in the function module. The algorithm is built within the Simulink environment, as shown in Fig. 9.

According to the simulation model established above and the data in Fig. 9, the comparison diagram of the waveform in Fig. 10 can be obtained. The results show that the feedforward control method of the adaptive neural network based on *e* correction can effectively suppress the interference by more than 50%.

To facilitate the simulation and description, the current value of the DSP is compared after A/D conversion, as shown in Fig. 11. Figure 11a shows that the high-frequency fluctuation waveform is similar to a sawtooth wave, while Fig. 11b

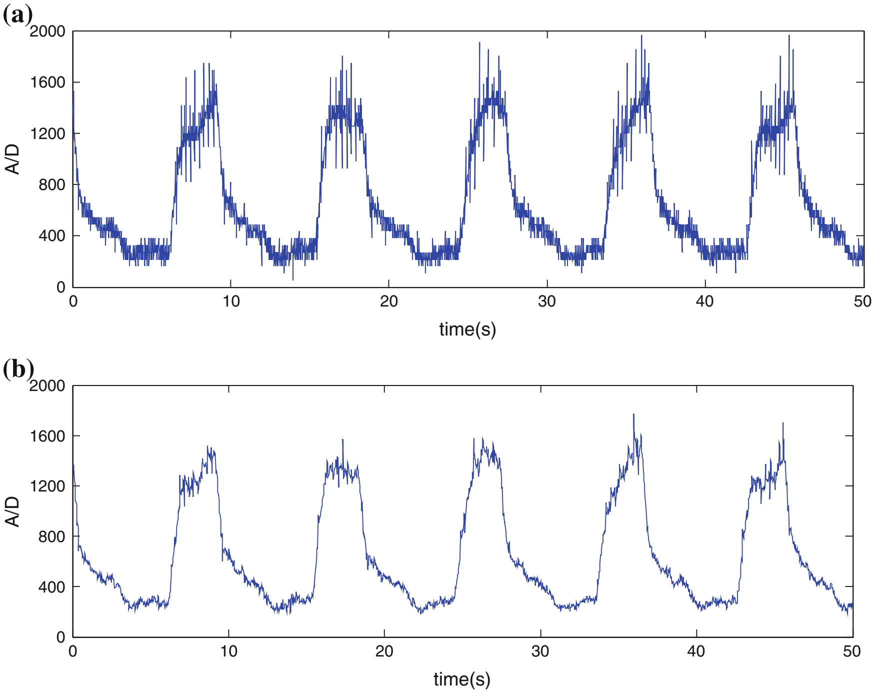

Fig. 11 Comparison of current waveform: **a** Actual waveform. **b** Waveform of adaptive neural network feedforward control based on modified *e* method

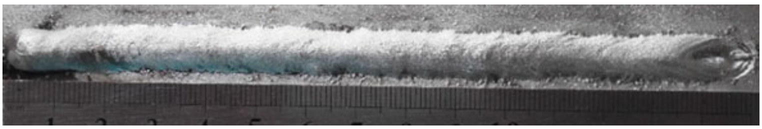

Fig. 12 Single pulse welding experiment

shows the anti-jamming waveform with adaptive neural network feedforward control based on modified *e* method. Results indicates that the feedforward control method of the adaptive neural network based on e correction can effectively suppress the interference.

The single pulse welding experiment was carried out using the above anti-interference control. The experimental parameters were as follows: the pulse peak current $I_p = 240$ A, the peak time $t_p = 3$ ms, the pulse base current $I_b = 53$ A, the base value time $t_b = 12$ ms, and a welding speed of 0.5 m/min. Figure 12 shows the weld appearance by single pulsed welding with the proposed control algorithm. Results indicates that the proposed control algorithm can be used to obtain high quality welds.

5 Conclusion

1. Based on the modeling and simulation of PID control, the optimal parameters are determined to be $k_p = 2.2$, integral time constant $T_I = 3$, and differential time constant $T_D = 20$. Furthermore, the current value of the DSP is processed for anti-jamming using a combination of the optimal PID controller and the adaptive neural network e correction method of feedforward control.
2. Pulse frequency modulation is employed in the process of welding arc length adjustment, which returns the arc length back to its original length faster than controlled variation of the external characteristics of the constant current.

References

1. Morimoto K, Doi T, Manabe H et al (2006) Advanced high power DC-DC converter using a novel type voltage source full-bridge soft-switching PWM inverter with high frequency transformer link for arc welding applications. IEEE Trans Ind Appl 126(3):237–247
2. Liu JK (2016) Advanced PID control MATLAB simulation, 4th edn. Publishing House of Electronics Industry, Beijing
3. Liao TF (2016) Study on waveform modulation method and process mechanism of double pulse MIG welding of aluminum alloy. Dissertation, South China University of Technology
4. Wei ZH (2012) Research on current waveform regulation of sinusoid modulated pulse MIG welding in aluminum alloy and expert system. Dissertation, South China University of Technology
5. Yao P (2012) Intelligent control strategy and process performance evaluation method for integrated twin wire arc welding power source. Dissertation, South China University of Technology
6. Wen D, Dong L (2009) MATLAB simulation of process control system. China Machine Press, Beijing
7. Zhao L (2015) Artificial neural network technology and its application. Electron Technol Softw Eng 2015(2):29–29
8. Liu XY, Liu H (2008) Artificial neural network and particle swarm optimization. Beijing University of Posts and Telecommunications Press, Beijing
9. Ren X, Lewis FL, Zhang J et al (2009) Feedforward control based on neural networks for hard disk drives. IEEE Trans Magn 45(7):3025–3030
10. Huang Y, Na J, Wu X et al (2015) Adaptive control of nonlinear uncertain active suspension systems with prescribed performance. ISA Trans 54:145–155
11. Li G, Na J, Stoten DP et al (2014) Adaptive feedforward control for dynamically substructured systems based on neural network compensation. IEEE Trans Control Syst Technol 22(3):944–954
12. Na J, Chen Q, Ren X et al (2014) Adaptive prescribed performance motion control of servo mechanisms with friction compensation. IEEE Trans Industr Electron 61(1):486–494